Biosensors and Bioelectronics 79 (2016) 574–580

Contents lists available at ScienceDirect

Biosensors and Bioelectronics

journal homepage: www.elsevier.com/locate/bios

Fe_3O_4@Ag magnetic nanoparticles for microRNA capture and duplex-specific nuclease signal amplification based SERS detection in cancer cells

Yuanfeng Pang [a,b], Chongwen Wang [b,c], Jing Wang [b,d], Zhiwei Sun [a,*], Rui Xiao [b,*], Shengqi Wang [b,*]

[a] Capital Medical University, Department of Toxicology, No. 10 Xitoutiao, You An Men, Beijing 100069, PR China
[b] Beijing Institute of Radiation Medicine, Beijing Key Laboratory of New Molecular Diagnosis Techniques for Infectious Dedication, 27 Taiping Road, Beijing, PR China
[c] College of Life Science &Bio-Engineering, Beijing University of Technology, Beijing 100124, PR China
[d] School of Pharmaceutical Science, Zhengzhou University, Zhengzhou 450001, PR China

ARTICLE INFO

Article history:
Received 28 September 2015
Received in revised form
16 December 2015
Accepted 17 December 2015
Available online 18 December 2015

Keywords:
MiRNA
Duplex-specific nuclease
Fe_3O_4@Ag
Paramagnetic
SERS

ABSTRACT

A functionalized Fe_3O_4@Ag magnetic nanoparticle (NP) biosensor for microRNA (miRNA) capture and ultrasensitive detection in total RNA extract from cancer cells was reported in this paper. Herein, Raman tags-DNA probes modified Fe_3O_4@Ag NPs were designed both as surface-enhanced Raman scattering (SERS) SERS and duplex-specific nuclease signal amplification (DSNSA) platform. Firstly, target miRNAs were captured to the surface of Fe_3O_4@Ag NPs through DNA/RNA hybridization. In the presence of endonuclease duplex specific nuclease (DSN), one target miRNA molecule could rehybrid thousands of DNA probes to trigger the signal-amplifying recycling. Base on the superparamagnetic of Fe_3O_4@Ag NPs, target miRNA let-7b can be captured, concentrated and direct quantified within a PE tube without any PCR preamplification treatment. The detection limit was 0.3 fM (15 zeptomole, 50 μL), nearly 3 orders of magnitude lower than conventional fluorescence based DSN biosensors for miRNA(~100 fM), even single-base difference between the let-7 family members can be discriminated. The result provides a novel proposal to combine the perfect single-base recognition and signal-amplifying ability of the endonuclease DSN with cost-effective SERS strategy for miRNA point-of-care (POC) clinical diagnostics.

1. Introduction

MicroRNAs (miRNAs) are a class of small-sized (~22 nucleotides), noncoding, single-stranded RNA molecules that play an important regulatory role in the expression of diverse genes by leading mRNA degradation or translational inhibition at the post-transcriptional level in a sequence-specific manner (Novina and Sharp, 2004; He and Hannon, 2004), miRNAs control several biological processes particularly regulatory pathways during development, apoptosis, cell proliferation and differentiation, organ development and cancer so that miRNAs are used as biomarkers for various diseases especially in the diagnosis of various types of cancers (Yanaihara et al., 2006; Kilic et al., 2012; Farazi et al., 2011). Consequently, the development of rapid and sensitive methods for identification and quantification of miRNAs is highly desirable in biomedical research and clinical diagnosis. However, due to their unique characteristics, including small size, sequence homology among family members, low abundance in total RNA samples and susceptibility to degradation, it is hard to identify and quantify miRNAs by using the common nucleic acid detection methods such as Northern blotting (Lagos-Quintana et al., 2001) (hundreds of micrograms of total RNA required), microarrays (Thomson et al., 2004) (cross hybridization of the homology miRNA family members and poor reproducibility) and real-time quantitative polymerase chain reaction (qRT-PCR) (Chen et al., 2005) (hard to design of the primers as the short length of miRNA). Moreover, the long analysis time for these methods ranging from several hours (PCR) to days (microarray) also makes them impractical in point-of-care (POC) clinical settings.

Recent years, an increasing attention has been paid to the development of different isothermal amplification techniques for miRNA detection (Liu et al., 2012; Zhang and Zhang, 2012; Liu et al., 2013; Zhu et al., 2013). During which, Jia et al., (2010) applied an exponential amplification reaction (EXPAR) method to miRNAs detection with detection limit of about 15 aM. Zhang and Zhang (2012) reported a single-quantum-dot based EXPAR

* Corresponding authors.
E-mail addresses: zwsun@ccmu.edu.cn (Z. Sun), Ruixiao203@sina.com (R. Xiao).

http://dx.doi.org/10.1016/j.bios.2015.12.052
0956-5663/

nanosensor and the detection limit reached an amazing 0.1 aM. However, the nonspecific background amplification in both thermal cycling and isothermal processing formats of EXPAR was an interference espacially in practical samples. To solve the nonspecific background amplification problem, the signal-amplifying mechanism of duplex-specific nuclease signal amplification (DSNSA) has been adopted for miRNA detection. In 2002, DSN was found to be able to cleave DNA–DNA duplex or DNA in DNA–RNA heteroduplexes (Shagin et al., 2002). Moreover, this enzyme shows a good specificity capability to discriminate between perfectly and no perfectly matched with one mismatch in DNA–DNA duplex (at least 10 bp) or DNA–RNA heteroduplexe (at least 15 bp). So far, several DSN signal amplifying mechanism based biosensors for miRNAs have been reported. Yin et al. (2012) firstly applied the DSN for miRNA detection, by using fluorescence Taqman probes, miR-141 has been detected and the limit of detection (LoD) was 100 fM. In 2014, Xi et al. (2014) reported a DSN based miR-21biosensor which combined WS_2 nanosheet as fluorescence quencher therefore the expensive Taqman probes can be replaced by cheaper one-terminal fluorophore labeled DNA probes (LoD~300 fM). Degliangeli et al. (2014) reported a DNA probes functionalized Au NP as DSN signal amplification and fluorescence quenching substrate based on which cancer-related miR-21 (LoD~5–8 pM) and miR-203(LoD~25 pM) could be absolutely quantified in total RNA extract from cell cultures.

However, even with rigorous target selectivity and negligible nonspecific background amplification, the sensitivity of fluorescence DSN biosensor (pM-100 fM) was worse compared with EXPAR biosensors(~aM). On the other hand, the fluorescent tags of the DSN-based miRNA biosensors were highly susceptible to photobleaching and exhibited broad-spectrum emissions easy to overlap (Mehta et al., 1999). In this case, the multiple miRNAs analysis in practical samples may be limited by diverse excitation wavelength, signals cross-interference between fluorescence labels and high background signal in practical samples. Here, we use surface-enhanced Raman scattering (SERS) as signal reporter because it offers a unique "signature" spectrum profile for individual Raman dye and provides the opportunity for multiplex assay detection with a single excitation wavelength in a low-cost and portable Raman microscope, which is an expected diagnostic devices for POC testing in family (Mabey et al., 2004). Especially with the development of nanotechnology, various nanostructured metallic (e.g. Silver and gold) nanorod or nanoparticles (NPs) have been applied as hybridization SERS substrate for miRNA detection in the sample solution (Ye et al., 2014; Guven et al., 2014). However, magnetic nanoparticles based miRNA SERS biosensor has never been reported before.

In our system, a functionalized Fe_3O_4@Ag magnetic nanoparticle has been designed as miRNA capture and DSN signal amplification platform for SERS detection. The Fe_3O_4@Ag serves both as SERS and concentration tool. MiRNA detection is demonstrated here by the DSN hydrolyzed the DNA probes of the DNA/RNA duplex, therefore, Raman tags could diffuse away from the Ag surface and induce a Raman intensity attenuation. Based on the Fe_3O_4@Ag NPs, miRNAs capture, concentration and direct quantification can be finished within a PE tube without any PCR pretreatment. Previous studies have reported the DSN based fluorescence biosensor (Yin et al., 2012; Xi et al., 2014) for miRNA or Fe_3O_4@Au based SERS biosensor for DNA sequence (Zhang and Zhang, 2012), however, the Fe_3O_4@Ag based miRNA biosensor with the merit of DSN signal amplification has never been combined for miRNAs identification and quantification. It may provide a novel exploration for miRNA related cancers POC diagnosis.

2. Experimental

2.1. Materials and instrumentation

Silver nitrate, Ferric chloride ($FeCl_3 \cdot 6H_2O$), Ethylene glycol, Polyethyleneimine branched (PEI, MW 25000), Polyvinylpyrolidone (PVP, MW 40000), N-Hydroxysuccinimide (NHS), 1-ethyl-3-(3-dimethylaminopropyl)-carbodiimide(EDC), 11-mercaptoundecanoic acid (MUA), 11-mercapto-1-undecanol ethanolic (MU) were purchased from Sigma-Aldrich (St. Louis, MO). and all other chemicals were purchased from Shanghai Chemical Reagent Co. (Shanghai, China). The let-7 miRNAs and Cy3-labeled DNA probe were ordered from IDT, Inc. (Coralville, IA) and the sequences are given in Table S1. Duplex-specific nuclease (DSN) and the master buffer were purchased from Evrogen Joint Stock Company (Moscow, Russia). All reagents were of analytical grade and were used without further purification. Transmission electron microscope (TEM) images were taken on a Hitachi H-7650 TEM at an accelerating voltage of 200 kV. Scanning electron microscope (SEM) was performed with a JEOL JSM-7001F microscopy at an accelerating voltage of 5 kV. Raman spectra was recorded on a portable Raman system (B&W Tek, i-Raman Plus BWS465-785H spectrometer) with 785 nm laser excitation.

2.2. Preparation of monodispersed Fe_3O_4@Ag core–shell microspheres

Firstly, the Fe_3O_4 magnetic particles (400 nm) were synthesized through a modified solvothermal reaction as previously reported (Li et al., 2013). Secondly, Fe_3O_4@PEI microspheres were synthesized through a PEI self-assembly process by dispersing 0.2 g Fe_3O_4 microspheres in the PEI solution (0.25g/50 mL) under sonication for 2 h. After well prepared, PEI-modified Fe_3O_4 microspheres were mixed with colloidal 3 nm Au NPs and sonicated for 1 h to form Fe_3O_4@PEI@Au NPs. Finally, 10 mg Fe_3O_4@PEI@Au NPs was dispersed in 100 mL 0.25 mM silver nitrate aqueous solution containing 0.2 wt% PVP, then excessive amount of 37% formaldehyde (150 μL) and 25% ammonia solution (300 μL) were added in sequence. The Fe_3O_4@Ag core–shell microspheres were obtained within 2 min under sonication at 30 °C. The products were magnetically separated and rinsed five times with deionized water to remove the excess PVP.

2.3. Cy-3-DNA probes immobilized on Fe_3O_4@ Ag nanoparticles

The amino-terminated Cy-3-DNA was immobilized onto the surface of carboxylic-Fe_3O_4@Ag NPs followed the previous report with little modification (Li et al., 2012). Typically, the Fe_3O_4@Ag NPs were cleaned and incubated overnight in a solution containing 100 mM MUA and 100 mM MU for carboxylation. The resulting MUA/MU modified NPs were activated by immersion in a solution containing 50 mM NHS and 200 mM EDC then incubated overnight in a PBS solution containing 1 μM amino–DNA probes. After immobilization, the DNA–Fe_3O_4@Ag NPs were washed 3 times using deionized water and stored in 0.05 M sodium chloride, 50 mM Tris–HCl (pH 8.0). The number of coupled DNA per particle was calculated as 2.5×10^3 according to previous report (Pang et al., 2015).

2.4. MiRNAs SERS detection

The amplified detection of miRNAs was performed in a 50 μL reaction mixture containing 1 × DSN master buffer (50 mM Tris–HCl (pH 8.0), 5 mM $MgCl_2$ and 1mM DTT), 0.06 U μL^{-1} DSN, 0.5 U μL^{-1} RNase inhibitor, 10 pM DNA-Fe_3O_4@Ag NPs. Let-7 miRNAs of different concentrations were added to the solution and

incubated at 55 °C for 60 min. Finally, the magnetite microspheres complex were washed and separated from the solution and then concentrated under the Raman laser through a magnet for SERS detection.

2.5. Cell culture and sample preparation

HeLa cells, A549 cells, and MCF-7 cells were cultured in Dulbecco's Modified Eagle Medium (DMEM) supplemented with 10% fetal bovine serum and 100 U mL^{-1} penicillin–streptomycin at 37 °C in a humidified 5% CO_2 incubator. The small RNA was extracted from cultured cancer cells by a RNA extraction kit from Takara (RNAiso for small RNA) according to the manufacturer's specification procedures.

3. Results and discussion

3.1. Operating principle illustration and Fe_3O_4@Ag nanoparticles characterization

The assay strategy is illustrated in Scheme 1. Raman tag Cy3 labeled DNA probes (Cy3-DNA) were immobilized on the surface of Fe_3O_4@Ag thus obvious surface enhance Raman scattering signal can be induced by the rough Fe_3O_4@Ag surface (Kuhn et al., 2006). Upon target miRNAs added, the fixed complementary DNA probes could capture and hybridize the target miRNAs to form DNA/RNA heteroduplex. With DSN, DNA probes of the DNA/RNA can be hydrolyzed and the Cy3 Raman tags in the DNA fragments were released from the Fe_3O_4@Ag surface, therefore, the intensity decreasing of Raman signal happened. This process can be recycled by one target miRNA cleaving thousands of DNA probes (Yin et al., 2012) so that significant signal amplification can be expected. After the signal amplification, the samples were concentrated by a magnet, the Cy-3-DNA fragments can be washed away and SERS signal was recorded. As the Fe_3O_4@Ag complex was focalized under the Raman laser, the sensitivity was increased largely. Herein, the intensity attenuation was directly related to the amount of the target miRNA.

The characters of Fe_3O_4@Ag NPs are demonstrated in Fig. 1. As shown in the TEM photographs (Fig. 1a), firstly, paramagnetic Fe_3O_4 microspheres with a diameter of approximately 400 nm were synthesized. Secondly, in order to harvest complete and uniform Ag shell with high roughness, we used a "seed-mediated growth" method by coating the Fe_3O_4 microspheres with 3 nm Au seed through hydrophilic PEI self-assembled on the surface of Fe_3O_4 microspheres as inker, therefore Au seeds can be immobilized on the surface of the Fe_3O_4 microspheres by covalent binding between the $-NH_2$ groups of the PEI (Fe_3O_4@PEI@Au). Finally, Ag^+ was reduced and deposited on the Au seeds, resulting in complete Ag shell surrounding the Fe_3O_4 core with continuous and rough edges(~30 nm). The magnetic properties of the Fe_3O_4@Ag core–shell NPs were investigated using a superconducting quantum interference device magnetometer (SQUID, MPMSXL-7) at 300 K, as shown in Fig.1b, the saturation magnetization (MS) of the Fe_3O_4, Fe_3O_4@Au seeds, Fe_3O_4@Ag shell NPs were founded to be 79.1, 69.5 and 59.5 emu g^{-1}, respectively. Compared with the recently reported magnetic metal NPs based SERS sensors (e.g. Fe_3O_4@SiO_2@Ag NPs or Fe_3O_4@C@Ag NPs) with about 60% magnetic saturation values decreasing (Wang et al., 2013; Ge et al., 2008), the MS for our Fe_3O_4@Ag nanoparticles decreased only about 25%, moreover, all of the curves nearly intersect with the origin, which showed that all of the three products were in a superparamagnetic state at room temperature (Prigodich et al., 2011). It proved that our Fe_3O_4@Ag microspheres possess both good disparity and strong magnetic responsiveness. In the practical separation test (Fig. 1b), the Fe_3O_4@Ag could be completely separated from the solution within only 10 s when the magnetic field was applied. Such a short separation time reflects the potential of these magnetic nanoparticles for the target rapid separation and concentration for SERS detection.

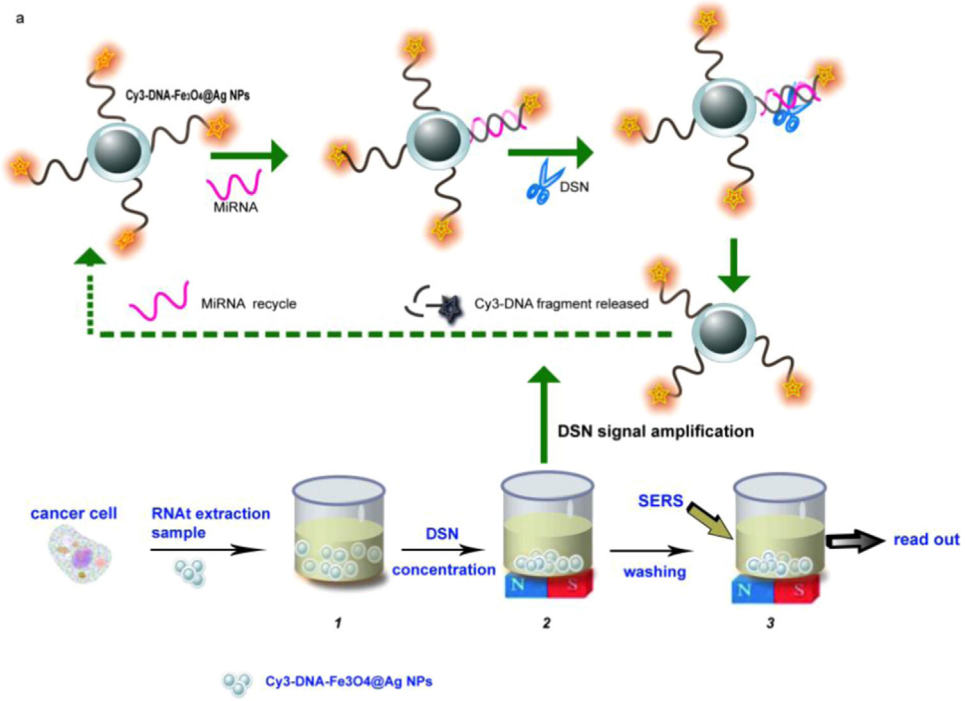

Scheme 1. Schematic illustration of miRNA assay strategy. (1) mix RNAt sample with Cy-3-DNA modified Fe_3O_4@Ag NPs (2) concentrate samples by a magnet and add DSN for incubation (3) wash away the Cy-3-DNA fragments and read out Raman signal.

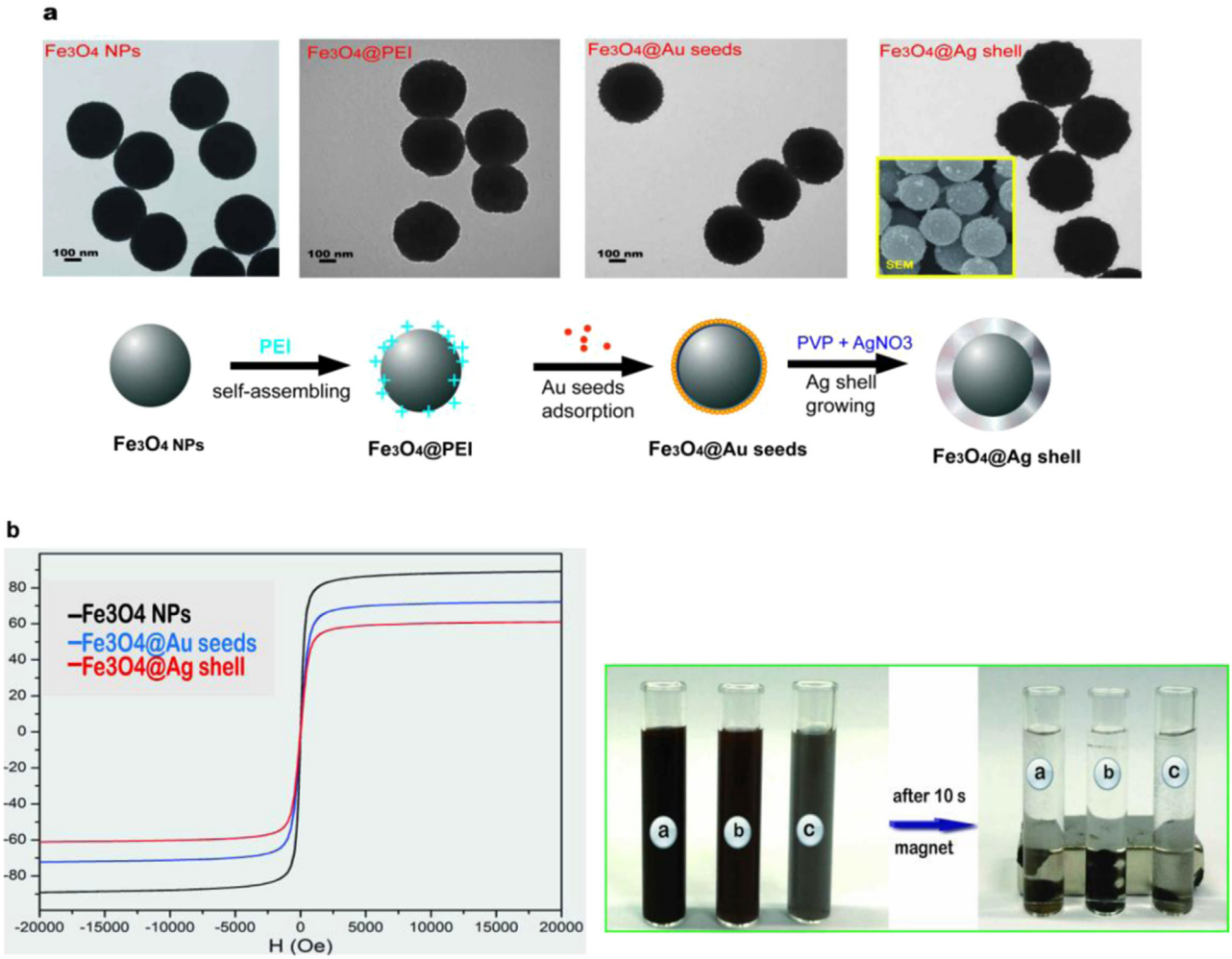

Fig. 1. (a) The Fe_3O_4@Ag NPs synthesis procedure and the corresponding TEM imagines, (b) Magnetic hysteresis curves of Fe_3O_4 NPs, Fe_3O_4@PEI@ Au seeds and Fe_3O_4@Ag shell and the corresponding magnetic separation behaviors photos at 300 K.

3.2. *Principle feasibility verification*

Although the DSN cleaving ability to the DNA probe in the DNA/RNA duplex free in the solution has been proved (Yin et al., 2012), the activity of DSN could be inhibited when oligonucleotides were immobilized on nanoparticles (Seferos et al., 2009). In 2014, Degliangeli group reported that DSN still kept enzymatic activity to the DNA probe in DNA–RNA heteroduplexes immobilized on the Au NPs (Degliangeli et al., 2014). Herein, the activity of DSN to the DNA probe in the DNA/RNA duplex immobilized on the Fe_3O_4@Ag NPs was investigated firstly. Considering the significant roles of miRNA let-7b in cellular processes and human diseases (Cheng et al., 2012) , it was selected as a model analyst and the Raman intensity at 1586 cm^{-1} (Cy3) was selected as the characteristic SERS signal for quantification. For the DSN cleaving ability experiment (Fig. 2a), the SERS intensity was almost the same for the DNA–Fe_3O_4@Ag NPs complex solution (Fig. 2a, curve a), DNA–Fe_3O_4@Ag NPs and DSN in 1 × DSN master buffer (Fig. 2a, curve b), DNA–Fe_3O_4@Ag NPs and let-7b mixture solution (Fig. 2a, curve c). However, the SERS intensity decreased largely when let-7b was added to the DNA–Fe_3O_4@Ag NPs and DSN mixture system after incubation for 60 min (Fig. 2a, curve d). This comparison indicated that the SERS signal attenuation was indeed triggered by let-7b due to the DSN efficiently hydrolyzing DNA probe in the immobilized DNA/RNA heteroduplexes, but not by the DSN reaction with probe DNA immobilized on the Fe_3O_4@Ag NPs only. The obvious signal decreasing indicated that DSN still kept enough activity to DNA probes on the surface of the Fe_3O_4@Ag NPs.

The enzymatic activity processing was also investigated and the result is shown in Fig. 2b. The SERS intensity decreased rapidly after the whole system was incubated from 0 to 60 min, afterwards, the decreasing turned to inconspicuous and reached a plateau at approximately 120 min, which indicated an effective total digestion of the immobilized probes. Due to previous reports, the DSN cleavage reaction can be finished within 30 min for DNA probes in DNA/RNA duplex free in the solution (Shagin et al., 2002; Yin et al., 2012). For our system, the cleavage reaction rate was lower. The probable reason was that the nucleases enzymatic activity was inhibited through the high local salt concentration around the nanoparticle surface (Degliangeli et al., 2014; Ren et al., 2013). Here, for our system, the buffer with 0.05 M NaCl was suitable to keep the cleavage reaction rate and an incubation time of 60 min was sufficient to maximize the sensitivity and lower the cost.

3.3. *Absolute quantification and single-nucleotide discrimination of miRNA let-7b from the let-7 family members*

In order to achieve the best assay performance, we firstly optimized the amplification and sensing conditions including the amount of DSN and the working temperature in the DSN signal amplification reaction. The SERS intensity with various

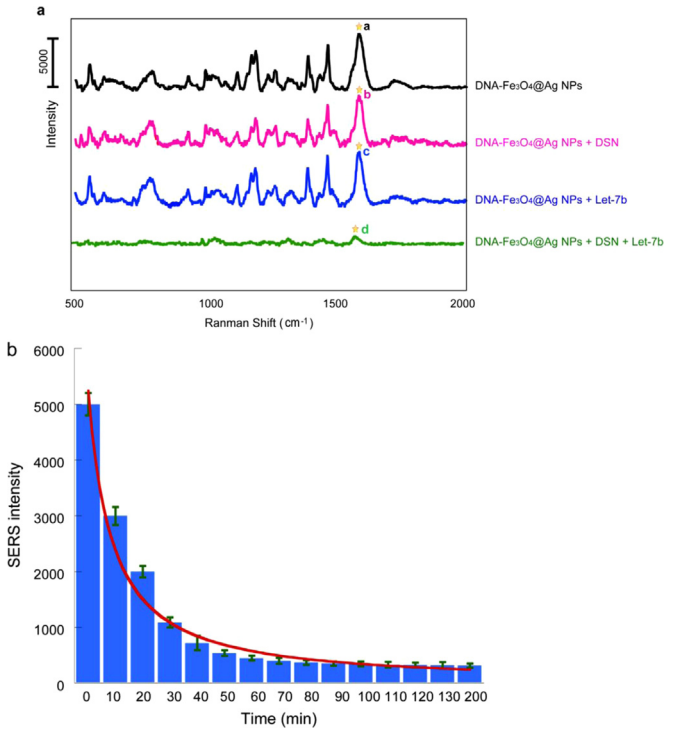

Fig. 2. (a) SERS spectra of DNA–Fe_3O_4@Ag NPs (curve a), DNA–Fe_3O_4@Ag NPs and DSN solution (curve b), DNA–Fe_3O_4@Ag NPs and let-7b solution (curve c), DNA–Fe_3O_4@Ag NPs plus let-7b and DSN solution (Curve d). (b) Enzymatic processing monitoring of DSN in the DNA–Fe_3O_4@Ag NPs plus let-7b solution. (10 pM of DNA–Fe_3O_4@Ag NPs (~2.5×10^3 DNA/NP), 0.06 U μL^{-1} of DSN,10 nM target let-7b in 1 × DSN master buffer (50 mM Tris–HCl (pH 8.0), 5 mM $MgCl_2$ and 1 mM DTT), 0.05 M Na^+,0.5 U μL^{-1} of RNAse inhibitor). Error bars are standard deviation of three repetitive experiments. The DSN enzymatic activity kinetic curve was fitted by Origin 8.5 non-line curve fit tool.

concentrations of DSN were recorded in Figure S1a (Supporting Information), the highest Raman intensity ratio (R_0/R, where R_0 and R are the Raman signals in the absence and the presence of miRNA) was observed when DSN was 0.06 U μL^{-1}, therefore, this value was set as optimal DSN concentration for the subsequent experiments. The reaction temperature was also optimized and the highest R_0/R was observed when the temperature was 55 °C, therefore, the incubation temperature was set to 55 °C (Figure S1b). For the cost-effective purpose, a period of 60 min incubation at 55 °C with 0.06 U μL^{-1} DSN was sufficient for the detection. Under optimized test conditions, the performance of the strategy for quantitative analysis of miRNA let-7b was investigated. By measuring the Raman intensity at 1586 cm^{-1}, we quantitatively analyzed the variance of Raman intensity with the concentration of let-7b. As shown in Fig. 3a, the SERS signal decreased with the concentration of let-7b from 1 pM to 10 nM and showed good linear fit to the concentration of let-7b in the range from 0 to 1000 pM with a correlation coefficient 0.998. The detection limit was 0.3 fM (15 zeptomole, 50 μL) which was estimated by the equation $LOD = 3 \times S_{blank}/m$, in which S_{blank} and m were the standard deviation of the blank and the slope obtained from the linear fitting. The limit of detect was decreased nearly 3 orders of magnitude as compared with the DSN based fluorescence miRNAs sensors (Yin et al., 2012; Xi et al., 2014; Degliangeli et al., 2014), as much as 6 orders of magnitude as compared with the SERS-based direct assay (Guven et al., 2014) and 5 orders of magnitude as compared with the p19-based magnetobiosensors (Campuzano et al., 2014), 3 orders of magnitude as compared with the EXPAR-based electrochemical biosensor (Yan et al., 2013) and an equal sensitivity to the EXPAR-based SERS method (Ye et al., 2014).

Compared with the common SERS biosensor, our DSN-based SERS method may discriminate target miRNA from the high sequence homology miRNAs and can be used to simultaneously detect multiple miRNAs in cancer cells. Notably, the zeptomole sensitivity permits the detection of miRNA transcripts (e.g. 10–100 copies per cell) from as little as 10,000–30,000 cells that can be harvested from clinical biopsies without prior PCR amplification (Stomper et al., 1998), therefore, the POC tests of disease-associated miRNAs clinical diagnosis can be expected.

As previous report (Arefian et al., 2011), the discrimination of miRNAs from sequence homology family members is important for understanding their biological functions and relationship with human diseases. However, it has been always challenging due to their high sequence similarity. To evaluate the specificity of our strategy, DNA probes complementary to let-7b were designed and immobilized on the Fe_3O_4@Ag NPs to distinguish let-7b from let-7 miRNA family members. As shown in Fig.3b, there was very slight signal change for all other let-7 family members except for let-7b (The corresponding SERS spectra are shown in the Supporting information, Fig.S2). It proved even for targets immobilized on the NPs, DSN still kept the one-base mismatch recognition ability no

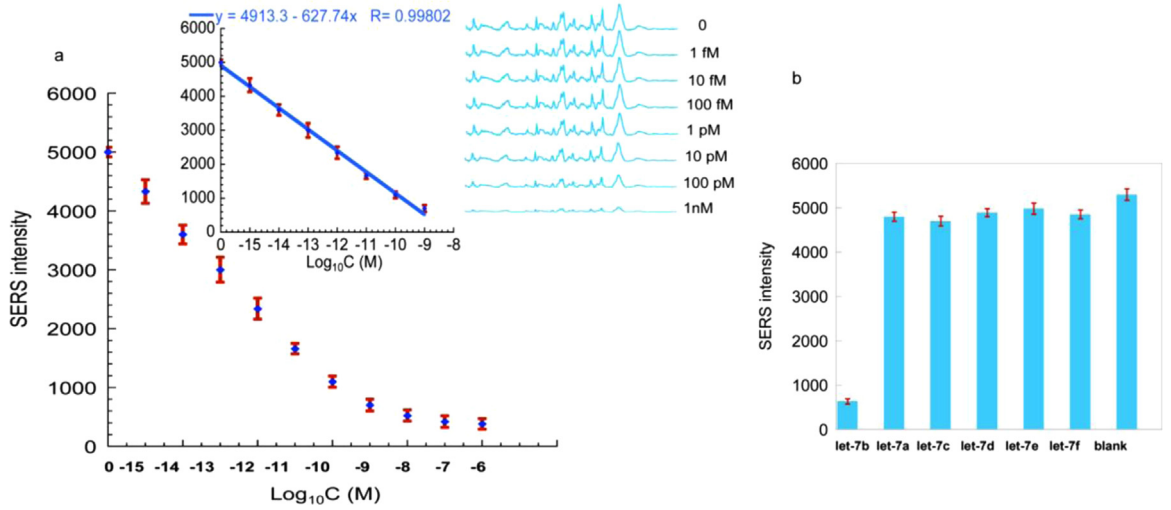

Fig. 3. (a)SERS intensities (1586 cm^{-1}) versus let-7b concentrations in logarithmic scale. Inset: SERS spectra and linear relationship between the SERS intensity and the miRNA concentration. (b) Specificity of miRNA assay. Bars represent the SERS intensity upon the different miRNAs targets with the same concentration of 10 nM, respectively. Error bars are the standard deviation of three repetitive experiments. Error bars are standard deviation of three repetitive experiments.

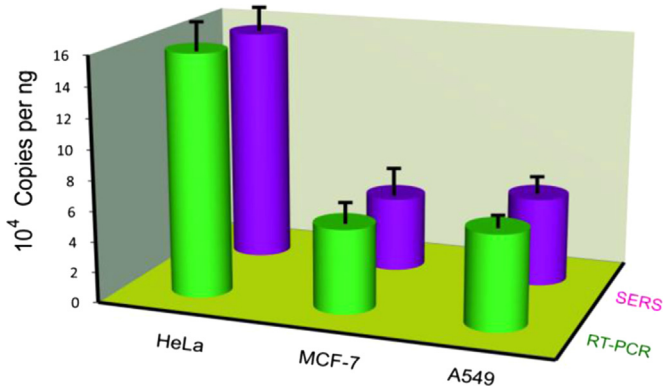

Fig. 4. Analysis of let-7b in total small RNA extracted from cultured cells by our SERS system and by a commercial qRT-PCR kit, respectively. The error bar indicates the standard deviation of three independent experiments.

Table 1
Comparison of the proposed SERS method and RT-PCR kit for the detection of let-7b in total RNA samples extracted from different cell lines.

Cell lines	HeLa	MCF-7	A549
SERS for let-7b (10^4 copies/ng total RNA)	15.9	5.5	6.2
RT-PCR for let-7b (10^4 copies/ng total RNA)	15.5	4.9	5.8
Relative error (%)	2.6	12.1	6.9

matter where the mismatched base was located. By using let-7 family as models, the highly sensitive mismatch discrimination ability for this assay was successfully demonstrated.

3.4. Feasibility investigation to real total RNA samples extracted from human cancer cell lines

Finally, to determine whether this method could be applied to real biological samples, we evaluated a testing for let-7b in total RNA sample extracted from different cell lines including the human breast cancer cell lines (MCF-7), cervical cancer cell lines (HeLa), and human lung adenocarcinoma cell lines (A549). The results indicated that Hela cell lines had higher let-7b expression level than A549 and MCF-7 cell lines (Fig. 4), which was in good accordance with previous reports (Nelson et al., 2004; Gao et al., 2013). The same samples were also analyzed by using TaqMan probes and commercial qRT-PCR kit (ordered from Life Technology, Applied Biosystems). As shown in Fig. 4, the results obtained by our strategy were in good agreement with those by qRT-PCR. The comparison of the determination results for these samples by using the commercial qRT-PCR kit and the proposed SERS method is shown in Table 1. It can be seen that the relative errors of the proposed SERS method compared to the commercial qRT-PCR method are less than $\pm$ 13%. We also determined the accuracy of the method by measuring the recovery of known amounts of let-7b spiked into the HeLa and MCF-7 cell lysates (Table S2 in the Supporting Information).The method also possessed good recovery rates of standard addition from 97% to 103%. These results indicated that our SERS approach is practical for miRNA absolute quantification in real samples.

4. Conclusions

In conclusion, we reported a DSN signal amplification based miRNA biosensor by using Fe_3O_4@Ag magnetic microsphere as SERS and enzyme hydrolysis platform. Through this method, the signal amplification and single-base discrimination ability of DSN were well combined with the high SERS performance of the Fe_3O_4@Ag. Moreover, the reproducibility and sensitivity were improved by the concentration ability of the paramagnetic Fe_3O_4@Ag NPs. It was preferable than the conventional Au or Ag NPs suspending in the solution for SERS detection, especially when the concentrations of NPs was quite low. By combining these advantages, miRNA let-7b can be discriminated from the let-7 family with a detection limit of 0.3 fM within a PE tube, which decreased 3 orders of magnitude as compared with the DSN-based fluorescence miRNA biosensors (Yin et al., 2012; Xi et al., 2014; Degliangeli et al., 2014). The low-cost Raman instrument, simple operation process and high sensitivity make our method a potential tool for miRNA related cancer POC diagnosis. In future studies, we will aim to apply our assay systems for multiplex cancer related miRNA samples real-time detection.

Acknowledgments

This work was supported by the Natural Science Foundation of China (No. 31100712), National 863 Key Project (2013AA020204), and Major Special Projects on Infectious Diseases (2013ZX10004802-008). The author of Y. Pang, C. Wan and J. Wang contributed equal to this research.

Appendix A. Supplementary material

Supplementary data associated with this article can be found in the online version at http://dx.doi.org/10.1016/j.bios.2015.12.052.

References

Arefian, E., Kiani, J., Soleimani, M., Shariati, S.A.M., Aghaee-Bakhtiari, S.H., Atashi, A., Gheisari, Y., Ahmadbeigi, N., Banaei-Moghaddam, A.M., Naderi, M., 2011. Nucleic Acids Res. 39, e80–e86.
Campuzano, S., Torrente-Rodrguez, R.M., Lopez-Hernandez, E., Conzuelo, F., Granados, R., Sanchez-Puelles, J.M., Pingarron, J.M., 2014. Angew. Chem. Int. Ed. 53, 6168–6171.
Chen, C.F., Ridzon, D.A., Broomer, A.J., Zhou, Z.H., Lee, D.H., Nguyen, J.T., Barbisin, M., Xu, N.L., Mahuvakar, V.R., Andersen, M.R., Lao, K.Q., Livak, K.J., Guegler, K., 2005. Nucleic Acids Res. 33, e179.
Cheng, J.C., Yeh, Y.J., Tseng, C.P., Hsu, S.D., Chang, Y.L., Sakamoto, N., Huang, H.D., 2012. Cell. Mol. Life Sci. 69, 2621–2633.
Degliangeli, F., Kshirsagar, P., Brunetti, V., Pompa, P.P., Fiammengo, R., 2014. J. Am. Chem. Soc. 136, 2264–2267.
Farazi, T.A., Spitzer, J.I., Morozov, P., Tuschl, T.J., 2011. Pathology 223, 102–115.
Gao, Z., Deng, H., Shen, W., Ren, Y., 2013. Anal. Chem. 85, 1624–1630.
Ge, J., Zhang, Q., Zhang, T., Yin, Y., 2008. Angew. Chem. 47, 8924–8928.
Guven, B., Dudak, F.C., Boyaci, I.H., Tamerc, U., Ozsozd, M., 2014. Analyst 139, 1141–1147.
He, L., Hannon, G.J., 2004. Nat. Rev. Genet. 5, 522–531.
Jia, H., Li, Z., Liu, C., Cheng, Y., 2010. Angew. Chem., Int. Ed. 49, 5498.
Kilic, T., Topkaya, S.N., Ariksoysal, D.O., Ozsoz, M., Ballar, P., Erac, Y., Gozen, O., 2012. Biosens. Bioelectron. 38, 195–201.
Kuhn, S., Håkanson, U., Rogobete, L., Sandoghdar, V., 2006. Phys. Rev .Lett. 97, 017402.
Lagos-Quintana, M., Rauhut, R., Lendeckel, W., Tuschl, T., 2001. Science 294, 853–858.
Li, J.M., Ma, W.F., You, L.J., Guo, J., Hu, J., Wang, C.C., 2013. Langmuir 29, 6147–6155.
Li, M., Zhang, J., Suri, S., Sooter, L.J., Ma, D., Wu, N., 2012. Anal. Chem. 84, 2837–2842.
Liu, H., Li, L., Duan, L., Wang, X., Xie, Y., Tong, L., Wang, Q., Tang, B., 2013. Anal. Chem. 85, 7941–7947.
Liu, Y.Q., Zhang, M., Yin, B.C., Ye, B.C., 2012. Anal. Chem. 84, 5165–5169.
Mabey, D., Peeling, R.W., Ustianowski, A., Perkins, M.D., 2004. Nat. Rev. Microbiol. 2, 231–240.
Mehta, A.D., Rief, M., Spudich, J.A., 1999. J. Biol. Chem. 274, 14517–14520.
Nelson, P.T., Baldwin, D.A., Scearce, L.M., Oberholtzer, J.C., Tobias, J.W., Mourelatos, Z., 2004. Nat. Methods 1, 155–161.
Novina, C.D., Sharp, P.A., 2004. Nature 430, 161–164.
Prigodich, A.E., Alhasan, A.H., Mirkin, C.A., 2011. J. Am. Chem. Soc. 133, 2120–2123.
Ren, Y., Deng, H., Shen, W., Gao, Z., 2013. Anal. Chem. 85, 4784–4789.
Seferos, D.S., Prigodich, A.E., Giljohann, D.A., Patel, P.C., Mirkin, C.A., 2009. Nano

Lett. 9, 308–311.
Shagin, D.A., Rebrikov, D.V., Kozhemyako, V.B., 2002. Genome Res. 12, 1935–1942.
Stomper, P.C., Budnick, R., Stewart, C.C., 1998. Invest. Radiol. *33*, 51–55.
Thomson, J.M., Parker, J., Perou, C.M., Hammond, S.M., 2004. Nat. Methods 1, 47–53.
Wang, Y., Wang, K., Zou, B., GAO, T., Zhang, X., Dua, Z., Zhou, S., 2013. J. Mater. Chem. C. 1, 2441–2447.
Xi, Q., Zhou, D., Kan, Y., Ge, J., Wu, Z., Yu, R., Jiang, J., 2014. Anal. Chem. 86, 1361–1365.
Yan, Y.R., Zhao, D., Yuan, T.X., Hu, J., Zhang, D.C., Cheng, W., Zhang, W., Ding, S.J., 2013. Electroanalysis 25, 2354–2359.
Yanaihara, N., Caplen, N., Bowman, E., Seike, M., Kumamoto, K., Yi, M., Stephens, R. M., Okamoto, A., Yokota, J., Tanaka, T., Colin, G.A., Liu, C.G., Croce, C.M., Harris, C. C., 2006. Cancer Cell. 9, 189–198.
Ye, L., Hu, J., Liang, L., Zhang, C., 2014. Chem. Commun. 50, 12907–12910.
Yin, B., Liu, Y., Ye, B., 2012. J. Am. Chem. Soc. 34, 5064–5067.
Pang, F., Rong, Z., Wang, F., Xiao, R., Wang, S., 2015. Biosens. Bioelectron. 66, 527–532.
Zhang, Y., Zhang, C.Y., 2012. Anal. Chem. 2012 (84), 224–231.
Zhu, X., Zhou, X., Xing, D., 2013. Chemistry 19, 5487–5494.